

Threshold behavior of a driven incommensurate harmonic chain

S. N. Coppersmith and Daniel S. Fisher*

AT&T Bell Laboratories, 600 Mountain Avenue, Murray Hill, New Jersey 07974

(Received 25 May 1988)

The dynamics of a one-dimensional harmonic chain in the presence of a strong, incommensurate, sinusoidal potential and a uniform force F is investigated numerically. A threshold force F_T exists above which steady-state motion occurs. Near threshold, the linear and nonlinear responses of the system exhibit nontrivial critical behavior. Critical exponents describing the transition to a moving state are calculated, and scaling relations between them are conjectured.

I. INTRODUCTION

Although there has been enormous progress in understanding the complex dynamics of systems with a few dominant degrees of freedom,¹ much less progress has been made in understanding the nonlinear dynamics of systems in which infinitely many degrees of freedom play an essential role.² One of the simplest class of problems of this type is the collective motion of a large number N of interacting particles, each of which moves down its local potential gradient. Since this system is equivalent to motion of a single particle down an N -dimensional potential landscape, the motion has only trivial bifurcations for any finite N . However, as we shall see, the thermodynamic limit $N \rightarrow \infty$ can be very nontrivial. Examples of experimental realizations of this kind of phenomenon include collective transport of charge-density waves (CDW's) in the presence of disorder and flux lattice flow in dirty type-II superconductors.³

A. Model

The model we study is a driven dynamic generalization of the Frenkel-Kontorova model of a one-dimensional harmonic chain of particles in a periodic potential. It is described by an energy

$$U = \frac{1}{2} \sum_j (x_{j+1} - x_j)^2 - V \sum_j \cos x_j - F \sum_j x_j, \quad (1.1)$$

With an average particle spacing $2\pi\alpha$ enforced by the boundary conditions. We take simple relaxational dynamics

$$\frac{dx_j}{dt} = - \frac{\partial U}{\partial x_j} \quad (1.2)$$

and study the behavior as a function of the driving force F . In particular, we will be interested in the *average velocity* $v \equiv \langle dx_j/dt \rangle$ as a function of F , where the brackets denote a spatial and time average. We find that if the potential V is sufficiently large, a threshold F_T exists such that $v=0$ in steady state for $F < F_T$. We study critical behavior near this threshold numerically and by scaling arguments.

The properties of the model are most interesting for ir-

rational α , since otherwise, if the initial conditions are periodic, the motion for rational α reduces to a finite number of degrees of freedom with periodic boundary conditions. Following tradition, and motivated by a desire to stay as far as possible from such commensurate behavior, we will mostly focus on $\alpha = \phi \equiv (1 + \sqrt{5})/2$, i.e., the golden mean.

B. Outline

In the remainder of the Introduction, we briefly summarize earlier work on the properties of the model without a driving force, motivate the present work, and summarize our main results for the properties of the incommensurate system in the presence of a driving force, in particular, the behavior near the threshold force F_T . In Sec. II we discuss calculational methods, and Sec. III contains the detailed results. In Sec. IV we propose scaling laws, interpret the results, and compare them to those for other related models. Finally, in Sec. V we consider the applicability of the conclusions to experiments on CDW's.

Some of the work described here has been discussed in a previous brief communication by one of the authors.⁴

C. Zero driving force

The properties of Eq. (1.1) in the absence of a driving force ($F=0$) have been studied in detail by Aubry⁵ and others.⁶ In particular, if α is a "good" irrational,⁷ the properties of the ground state change dramatically as a function of V . For all V , Aubry has proven that the *ground states*, defined as having an energy which cannot be lowered by moving any finite collection of particles, can be described in terms of a *hull function* g , via

$$x_j = 2\pi\alpha j + \theta + g(2\pi\alpha j + \theta), \quad (1.3)$$

where g is periodic with period 2π and θ is a phase which labels the ground state. For rational α , θ only takes on discrete values but for irrational α , θ can take on any value. Note that as a consequence of Eq. (1.3), x_j is a quasiperiodic function of j . For good irrational α , g is a smooth function for V less than a critical value $V_c(\alpha)$, which for $\alpha = \phi$ (the golden mean) is found to be $V_c \approx 0.972$.⁸ As a consequence, for $V < V_c(\alpha)$ the ground

state for one value of θ can be continuously deformed into that for a different value of θ ; we call this region the *unpinned phase*. For $V > V_c(\alpha)$, on the other hand, the hull function develops an infinite number of discontinuities. The primary discontinuity corresponds to the maximum of the potential, i.e., x_j near an odd multiple of π , so that no particles lie within some distance of these potential maxima. This implies that the ground state cannot be smoothly evolved from one θ to another; we call this the *pinned phase*. In the pinned phase, there also exists metastability which is absent for $V < V_c$: a collection of nearby particles can be moved to a new metastable configuration with the effects of this change falling off exponentially at long distances. Thus, in many ways, the pinned incommensurate phase acts qualitatively more like the commensurate system, which is always pinned, while the incommensurate unpinned state acts more like the system in the absence of the periodic potential. For example, the spectrum of linear excitations about the ground state has long-wavelength modes down to zero frequency for $V=0$, and in the incommensurate unpinned phase there are analogous eigenmodes which simply involve slow variations of the phase θ . For the commensurate case and in the incommensurate pinned phase, on the other hand, there is a gap in the excitation spectrum.⁵

Near to the critical potential strength V_c , the system exhibits critical phenomena as studied in an earlier paper.⁹ For $V \lesssim V_c$, this is related to the breakdown of Kolmogorov-Arnol'd-Moser (KAM) trajectories for the extremal equations of Eq. (1.1) with $F=0$, considered as a map with j the time coordinate.^{8,10,11} We will not be concerned with this regime in the present paper.

D. Heuristics and summary of results

In the presence of an applied force, ground states are no longer defined, since the potential [Eq. (1.1)] is unbounded below. However, we can hope to adiabatically follow the metastable configurations which evolve from the ground states as F is increased from zero. For a commensurate system, it is straightforward to see that as long as $V > 0$, then for $F < F_T(V, \alpha)$, such metastable configurations exist, as can be seen for the trivial one-particle case with $\alpha=1$. Above F_T , however, no stationary solutions exist with average particle spacing $2\pi\alpha$.

As might be expected from the above discussion of the properties of ground states, the behavior for irrational α depends crucially on the strength of the periodic potential. For $V < V_c(\alpha)$, no stationary solutions exist for $F > 0$, as for the trivial $V=0$ case. The primary reason is as follows: For commensurate α , there is a gap in the excitation spectrum about the ground state, thus perturbation theory in F can be used to construct a nearby state. In the incommensurate unpinned phase, on the other hand, the presence of long-wavelength phononlike modes causes the perturbation expansion to break down. Physically, it is clear that, as for $V=0$, the system will start sliding for any $F > 0$. In fact, there is a linear response to the force so that $v \approx \sigma F$ for small F in the unpinned phase, as for $V=0$.¹²

In the pinned incommensurate phase, on the other

hand, perturbations about the $F=0$ ground state remain bounded, and there exist metastable configurations up to a threshold $F_T(V, \alpha)$, which approaches zero as $V \rightarrow V_c^+(\alpha)$. The point $V=V_c(\alpha)$, $F=0$ is thus a multicritical point.

What happens for $F > F_T$? As for the $V=0$ and unpinned incommensurate phases, we expect that the system will have a steady-state time-averaged velocity

$$\bar{v} \equiv \langle v(t) \rangle_t, \quad (1.4)$$

for $F > F_T$, where the brackets denote a time average. Far above threshold the effect of the potential is small and $\bar{v} \approx F$. For the commensurate system, which is effectively a finite collection of particles, the behavior near threshold is just that given by a simple saddle-node bifurcation:

$$\bar{v} \sim f^{1/2}, \quad (1.5)$$

where the reduced force f is defined as

$$f \equiv \frac{F - F_T}{F_T}. \quad (1.6)$$

As the denominator of a rational α grows, however, the regime of validity of Eq. (1.5) shrinks. For irrational α in the pinned phase, it is natural to expect that there will be a nontrivial critical exponent for the velocity:

$$\bar{v} \sim f^\zeta, \quad (1.7)$$

with $\zeta(\alpha) \neq \frac{1}{2}$ for irrational α . The hypothesis of nontrivial critical behavior is supported by the observation that a perturbation expansion in powers of the potential strength V for the incommensurate system diverges at threshold for $V > V_c$ because long-wavelength contributions become very large.

For $\alpha = \phi$ we find that with $V=4$, chosen to be far from both the critical V_c and ∞ , our numerical data are consistent with Eq. (1.7) with $\zeta = 0.67 \pm 0.05$. We also find support for the natural conjecture that the particle positions in steady state are again described by a hull function

$$x_j(t) = 2\pi\alpha j + \bar{v}t + g_+(2\pi\alpha j + \bar{v}t), \quad (1.8)$$

i.e., the same form as Eq. (1.3), but with the phase $\theta = \bar{v}t$ (plus a constant which can be removed by shifting the origin of time).¹³ For $F > F_T$, the hull function g_+ is continuous although its maximum derivative diverges as $F \rightarrow F_T^+$. We find that as $F \rightarrow F_T^+$ the dynamic hull function g_+ becomes equal to the discontinuous static hull function g for $F \rightarrow F_T^-$.

In addition to the critical behavior of \bar{v} for $F \rightarrow F_T^+$, we have investigated the critical behavior as $F \rightarrow F_T^-$ of various quantities, for example, the linear polarizability, defined as the change in the mean position $\langle \delta x_j(\omega) \rangle$ in response to a small ac applied force $\delta F(\omega)$ added to the dc force,

$$\chi(\omega) \equiv \frac{\langle \delta x_j(\omega) \rangle_j}{\delta F(\omega)}. \quad (1.9)$$

We find that $\chi_0 \equiv \chi(\omega=0)$ diverges as F nears F_T as

$$\chi_0 \sim |f|^{-\gamma}, \quad (1.10)$$

with $\gamma = 0.34 \pm 0.02$, and at threshold,

$$\chi(\omega) \sim \omega^{\rho-1}, \quad (1.11)$$

with $\rho = 0.33 \pm 0.04$. Various scaling laws will be suggested which relate these and other exponents to diverging characteristic lengths and times as $F \rightarrow F_T$.

E. Relationship to other models

The driven Frenkel-Kontorova model we study here is a particular limit of a class of models which have been studied in the context of sliding charge-density waves.¹⁴⁻¹⁶ These involve the motion of a harmonic lattice through a random rather than incommensurate potential. The simplest variant, which is related to the more realistic Fukuyama-Lee-Rice model,¹⁷ considers the phase ϕ_j of the charge-density wave at impurity j which has a preferred value $\beta_j[\text{mod}(2\pi)]$. If we write Eq. (1.1) in terms of the deviations from a uniform chain,

$$\phi_j \equiv x_j - \beta_j, \quad (1.12)$$

with $\beta_j = 2\pi\alpha_j$, then Eq. (1.1) is a special case of the general model¹⁸ with potential energy

$$U = \frac{1}{2} \sum_{[i,j]} J_{ij} (\phi_i - \phi_j)^2 - \sum_j V_j \cos(\phi_j - \beta_j) - F \sum_j \phi_j, \quad (1.13)$$

where the $J_{ij} > 0$ represent the stiffness of the CDW and the V_j the pinning strengths of the different impurity sites. Of particular interest are the cases where J_{ij} is short range in d dimensions and the β_j are random; however, these problems are very difficult to treat near the threshold, which is believed to exist for arbitrarily small disorder in any dimension.¹⁸ However, a limit in which considerable analytic progress can be made is that of infinite range J_{ij} , i.e., mean-field theory.^{18,19} In this limit, there is no spatial structure and thus a pseudorandom incommensurate β_j acts the same as a random β_j . So mean-field theory, in the special case that all the V_j are equal, is also equivalent to an infinite range incommensurate model.^{20,21} Although some of the behavior (particularly below threshold) does depend on the distribution of V_j , much of it does not.

In mean-field theory, it is found that a threshold F exists provided that at least some of the V_j are sufficiently large (greater than $\sum_i J_{ij}$). In this pinned phase, the velocity just above threshold obeys Eq. (1.7) with

$$\zeta_{\text{MF}} = \frac{3}{2}. \quad (1.14)$$

Thus, for zero dimensions, i.e., a finite number of degrees of freedom, $\zeta = \frac{1}{2}$, while in infinite dimensions, $\zeta = \frac{3}{2}$.

We would like to determine whether models with short-range interactions have critical behavior qualitatively similar to that of the mean-field theory, and if so, how the exponents describing the threshold are modified. In the absence of analytic progress for models of infinite size with finite range interactions, one is led to consider numerical investigations.

Computer simulations of randomly pinned one-dimensional chains¹⁴⁻¹⁶ suffer from three disadvantages stemming from computational limitations. First, one cannot distinguish a slowly moving chain from one that is relaxing into a stationary state in a finite but long time, so the threshold field cannot be determined accurately from a dynamic simulation. (This problem is related to the jerky motion found near threshold, which will be described in detail below.) This complication renders calculation of the exponent ζ in Eq. (1.5) extremely uncertain for random models. Second, finite-size effects are substantial. Littlewood¹⁶ has found that in simulations involving 200 impurities, one or two clumps of pinning sites appear to dominate the response near threshold. Sokoloff¹⁵ has examined larger systems (up to 5000 impurities), but the results still exhibit finite-size effects and the computations become very slow. Finally, averaging over different impurity configurations is time-consuming and it increases the uncertainties.

Incommensurate pinning allows one to avoid these problems. It is possible to find the threshold field using a static calculation, since the ground state of the system for $F=0$ appears to evolve continuously into the last metastable solution that disappears at $F=F_T$. Also, the regularity of the pinning makes it possible to investigate finite-size effects in a well-characterized way. No configurational averaging over different impurity distributions is needed, so only one calculation for each system size need be done.

Comparison of our results on the one-dimensional incommensurate chain with mean-field theory will be made in Sec. IV.

II. METHODS

The incommensurate limit can be approached numerically by examining a series of commensurate systems with mean particle spacing $2\pi\alpha_n$, where the α_n 's are optimal rational approximants to the irrational number α . The α_n 's are chosen in the standard manner using the continued fraction expansion of the irrational number α .⁷ For $\alpha = \phi = (\sqrt{5} + 1)/2$ the continued fraction consists of all 1's and the approximants are ratios of Fibonacci numbers: $q_n/p_n = \frac{1}{2}, \frac{2}{3}, \frac{3}{5}, \frac{5}{8}$, etc. Periodic boundary conditions determine the density for each system of p_n particles.

First, a static calculation was performed to find the threshold force F_T , and then dynamic simulations were done to characterize the velocity just above threshold. As mentioned above, any finite system is expected to exhibit finite-size behavior close enough to threshold,^{15,18,19} but by extrapolating the results for the α_n to $n \rightarrow \infty$, reliable information about the incommensurate limit can be obtained. It is necessary to work at V large enough so that a pinned phase exists; for our choice $\alpha = \phi$, the critical value $V_c \simeq 0.972$.⁸ Except where otherwise stated, the work described here was done with $V=4$, which is much larger than V_c but still of order unity. For this value of V , the correlation length associated with the pinning transition at $F=0$ and $V=V_c$ is slightly less than the interparticle spacing.

The determination of the threshold for a given system size was done in two steps. First the ground state of the system in zero field was found as in Ref. 9, using Newton's method to find a solution of the force equations while slowly increasing the potential strength V . Then the external force F was stepped by small increments δF and Newton's method was used to find static solutions of the force equations. If no solution was found, δF was halved and Newton's method attempted again. As discussed above, one expects there to be values of F for which no static solutions exist, and indeed there is a threshold value F_T above which no static solutions could be found using this technique. It is conceivable that for $F > F_T$ there are static solutions that are not obtained by adiabatically perturbing the $F=0$ ground state. However, the regularity of the pinning potential makes it plausible that the $F=0$ ground state remains the one of lowest energy for a given particle density and mean position even in the presence of a field and hence the one least likely to be destabilized by the external force. The consistency of the numerical results serves as a check of this assumption: Dynamic simulations for F decreasing towards F_T yield solutions that appear to approach the same configurations as those reached using static calculations with $F \rightarrow F_T^-$. It is this feature that enables one to make a quick and accurate determination of the threshold field.

For $F > F_T$ the particles move and the dynamics must be taken into account. In this region the equations of motion were solved using discretized time and a predictor-corrector routine to prevent numerical instabilities. The particles were started at equally spaced positions $x_j = 2\pi(q_n/p_n)j$ at time $t=0$ and their positions allowed to evolve until the transients decayed. This necessitates very long times for large systems near threshold—for instance, the equilibration time for an 89-particle system with $F=1.195$ ($f \approx 5 \times 10^{-3}$) exceeded 2000 time units. The steady-state positions of each particle were then calculated as functions of time. Other starting positions were found to yield the same steady state. The calculations were performed for various system sizes in order to extract properties of the incommensurate limit, $p_n \rightarrow \infty$.

III. RESULTS

A. Behavior below threshold

We first summarize the static results for $F < F_T$. As the force is increased, the configuration of the particles evolves smoothly until the metastable configuration disappears at threshold. For a given value of F , the positions x_j of all the particles are found to be given in terms of a periodic hull function $g(2\pi\alpha j; F)$ by Eq. (1.3); this was known to be the case for $F=0$.⁵ The hull function appears to evolve smoothly as a function of F up to F_T . Just as for the pinned state at zero field, g has an infinite number of discontinuities for all $F \leq F_T$. This situation is illustrated in Fig. 1. The behavior at threshold is in striking contrast to the continuous but self-similar hull function that is characteristic of the transition between

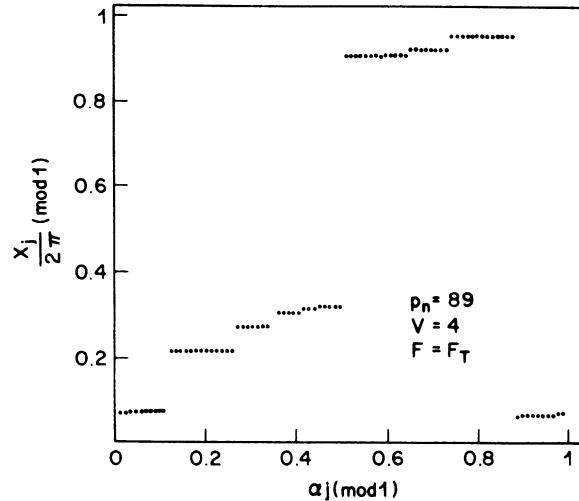


FIG. 1. Plot of the hull function $g/2\pi$, defined in Eq. (1.3) to be $(x_j/2\pi)(\text{mod } 1)$, which determines positions of the particles, as a function of $\alpha j(\text{mod } 1)$ for $V=4$ and $F \approx F_T \approx 1.1893$.

pinned and unpinned states at $F=0$ and $V=V_c$.¹⁰

The threshold force is remarkably insensitive to the system size. For a 21-particle system with $V=4$, $F_T(p_n)$ is equal to within the numerical error (10^{-7}) of that of 89 particles, and the threshold force for a five-particle system only differed by 0.2% from that of the largest system. The finite-size effects at $V=4$ are so weak that it is difficult to characterize them. In order to investigate them further, the threshold forces F_T for a smaller value of $V=1.5$ were found for $p_n=5, 8, 13, 21, 34, 55$, and 89. For this smaller value of V , the finite-size effects are larger, and only the difference in $F_T(p_n)$ between $p_n=55$ and 89 is within the error. Over the range studied, the deviation $\Delta F_n = F_T(p_n)/F_T(\infty) - 1$ does not appear to scale either as a power of p_n or exponentially in p_n . A good empirical fit was found to the form $\Delta F = A \exp(-Bp_n^C)$, with $A=14.7$, $B=0.97$, and $C=0.75$, as shown in Fig. 2. However, the uncertainty in the parameters is large, and no particular significance should be attached to this functional form.

In any case, the determination of the threshold force is straightforward and accurate since small systems can be used. For $V=4$, the threshold force approaches the asymptotic value $F_T = 1.189\,305\,32 \pm 10^{-7}$ as $p_n \rightarrow \infty$.

For each value of F the particles' positions were recorded and the spectrum of linearized excitations about the stationary configuration was obtained by diagonalizing numerically the matrix of force derivatives. At threshold the smallest eigenvalue remains of order 10^{-4} . This uncertainty is consistent with the uncertainty in the threshold field since the system is approaching a bifurcation point, where the smallest eigenvalue vanishes as discussed below.

An index m ranging from 1 to p_n labels the eigenvalues Λ_m and eigenvectors $\mathbf{u}_m(j)$. The index m is not simply a wave vector, although the phonons of the translationally invariant system ($V=0$) do evolve into the finite V excitations, albeit with some sort of singularity at $V=V_c$. The

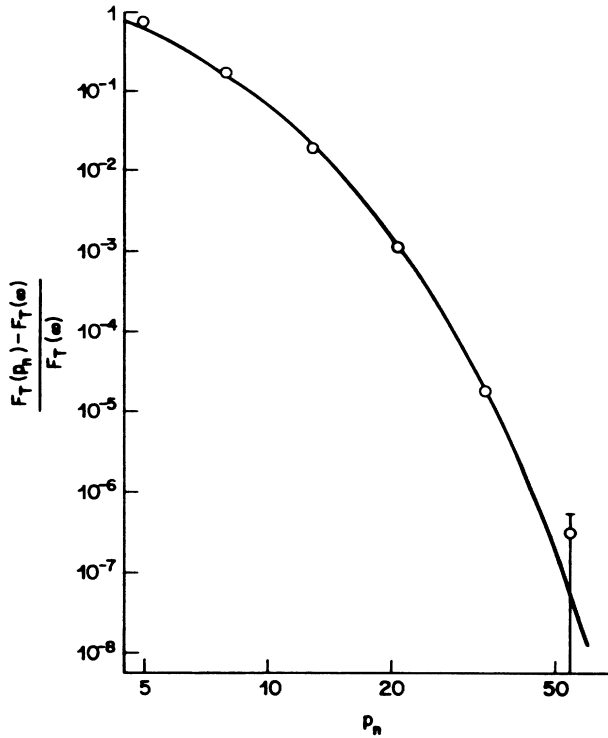


FIG. 2. Relative deviation of the threshold field for finite systems from its asymptotic value, $\Delta F_n = [F_T(n) - F_T(\infty)]/F_T(\infty)$, for $V=1.5$, plotted as a function of $p_n = 5, 8, 13, 21$, and 34 on a log-log scale. The solid line is a fit to the empirical form $\Delta F(n) = A \exp[-(B p_n^C)]$, with $A=14.7$, $B=0.97$, and $C=0.75$.

eigenmode spectrum Λ_m is shown for two values of the reduced force f on a log-log plot in Fig. 3. We see that the external force F induces qualitative changes in the spectrum. As F approaches F_T , the lowest eigenvalue Λ_1 appears to vanish as

$$\Lambda_1 \sim |f|^\mu, \quad (3.1)$$

with $\mu=0.5 \pm 0.005$ (Fig. 4), but there is a distribution of soft modes as the transition is approached. The low-lying eigenvalues with $\Lambda < 0.3$ correspond to highly localized eigenmodes; Fig. 5 demonstrates the localized nature of the three lowest eigenvectors of an 89-particle system. The higher modes do not appear localized, but we have not investigated them in detail.

As the threshold is approached, we expect the system to exhibit singular response at low frequencies. We have calculated the differential ac polarizability $\chi(\omega, F)$, which is the linear response to an additional uniform ac force $\delta F(\omega)$ as defined in Eq. (1.9). In terms of the eigenmodes and eigenvectors it is given by

$$\chi(\omega, F) = \lim_{n \rightarrow \infty} \sum_{m=1}^{p_n} \frac{\left[\sum_j u_m(j) \right]^2}{(-i\omega + \Lambda_m)}. \quad (3.2)$$

As $F \rightarrow F_T^-$, the dc polarizability is found to diverge as

$$\chi_0(f) \propto |f|^{-\gamma}, \quad (3.3)$$

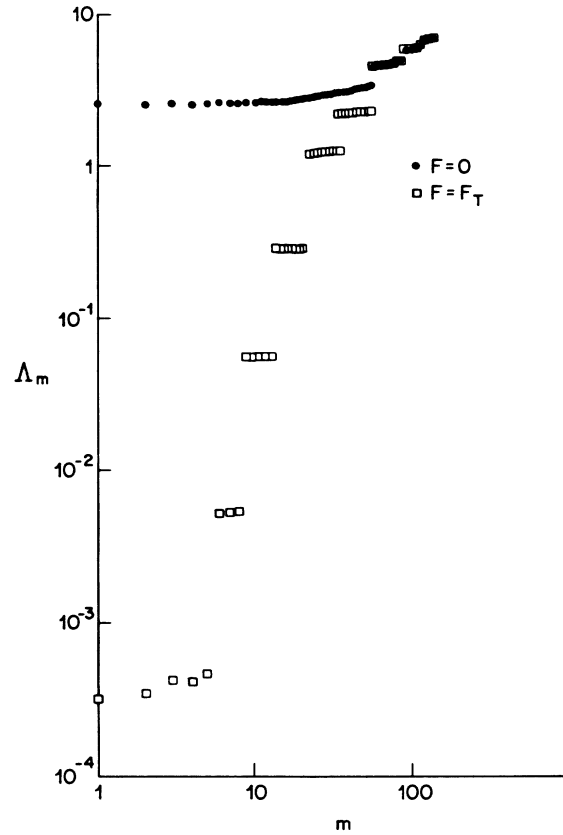


FIG. 3. Log-log plot of the phonon eigenvalues Λ_m as a function of m for $F=0$ and $F=F_T$, where m is an index labeling the Λ 's in ascending order. The field induces qualitative changes in the nature of the spectrum. Numerical errors cause the smallest eigenvalue at threshold to be nonzero.

with $\gamma=0.34 \pm 0.02$, as shown in Fig. 6. The polarizability plays the role of a divergent susceptibility at the threshold critical point. These results can be compared with the behavior for a finite number of degrees of freedom, for which $\gamma = \frac{1}{2}$ and $\mu = \frac{1}{2}$.

Below threshold the polarizability is analytic at low frequencies so that the ac conductivity

$$\sigma(\omega) \equiv -i\omega\chi(\omega) \quad (3.4)$$

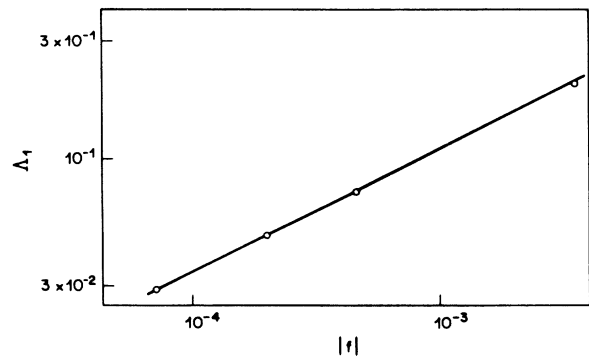


FIG. 4. Log-log plot of the lowest eigenvalue Λ_1 for a system with $p_n=89$ as a function of the reduced force $f = (F - F_T)/F_T$. The line is a fit with exponent $\mu=0.5 \pm 0.005$.

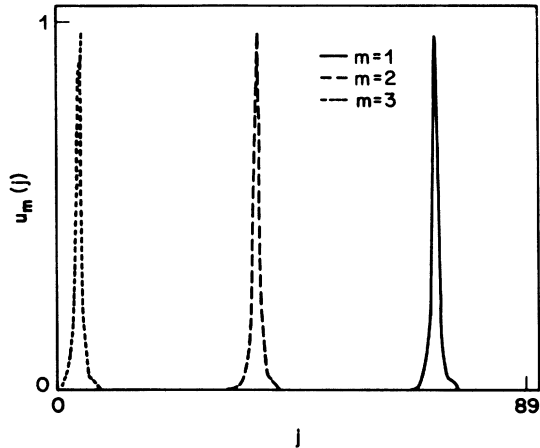


FIG. 5. Eigenvectors of the three lowest phonon modes $u_m(j)$ of an 89-particle system for $F \approx F_T$. The modes appear highly localized even at threshold.

has a real part which vanishes as ω^2 and an imaginary part equal to $-i\omega\chi_0$ for $\omega \rightarrow 0$. At threshold, $\sigma(\omega)$ is singular at low frequencies due to the low-lying eigenmodes, as shown in Fig. 7. We find that

$$|\sigma(\omega, F_T)| \propto \omega^\rho \tag{3.5}$$

for ω in the range $10^{-3} - 10^{-1}$, with $\rho = 0.33 \pm 0.04$. When ω is very small, we are limited by the numerical accuracy of the matrix diagonalization routines and deviation from the power-law behavior is found. The results for the 89- and 144-particle systems were basically identical in the range of frequency $10^{-4} < \omega < 10^{-3}$, so this discrepancy does not appear to be a finite-size effect. Therefore, although the results are consistent with power-law behavior, a firm conclusion cannot be reached on the basis of the data shown here. At large frequencies, $\sigma(\omega)$ at threshold is not qualitatively changed from its form at $F=0$, as can be seen from Fig. 8.

The gaps in the hull function g are associated with regions of the periodic potential in which there are no par-

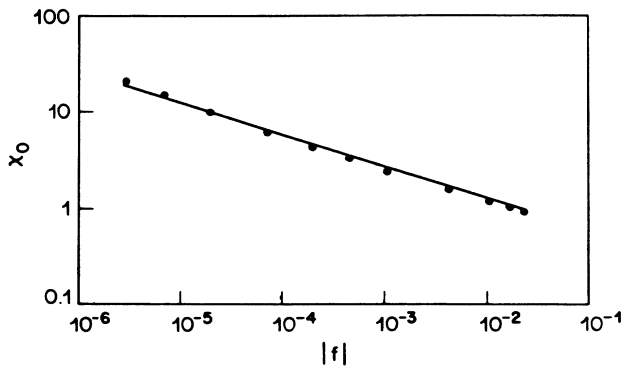


FIG. 6. Log-log plot of the polarizability $\chi_0(f)$ vs f for $f < 0$. The data are fit to the power law $\chi_0(f) \propto |f|^{-\gamma}$, with $\gamma = 0.34 \pm 0.02$.

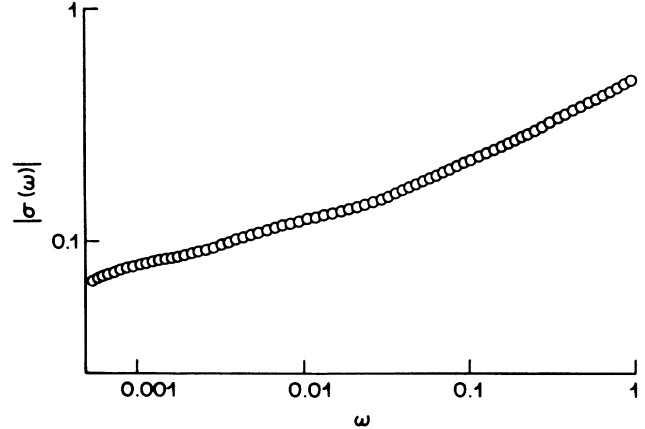


FIG. 7. Log-log plot of the absolute value of the ac conductivity at F_T , $|\sigma_{F_T}(\omega)|$, vs ω for small ω . The data are consistent with $|\sigma_{F_T}(\omega)| \propto \omega^\rho$ with $\rho = 0.33 \pm 0.04$ in the range $10^{-3} < \omega < 10^{-1}$. For $\omega < 10^{-3}$ numerical errors render the data unreliable.

ticles. For $F=0$, the largest gap corresponds to the absence of particles near the maxima of the potential. As mentioned above, even at threshold, there are regions where there are no particles. The size of the largest gap Δx is plotted as a function of f in Fig. 9; asymptotically, it appears to obey

$$\Delta x(F) \approx \Delta x(F_T) + A|f|^\nu, \tag{3.6}$$

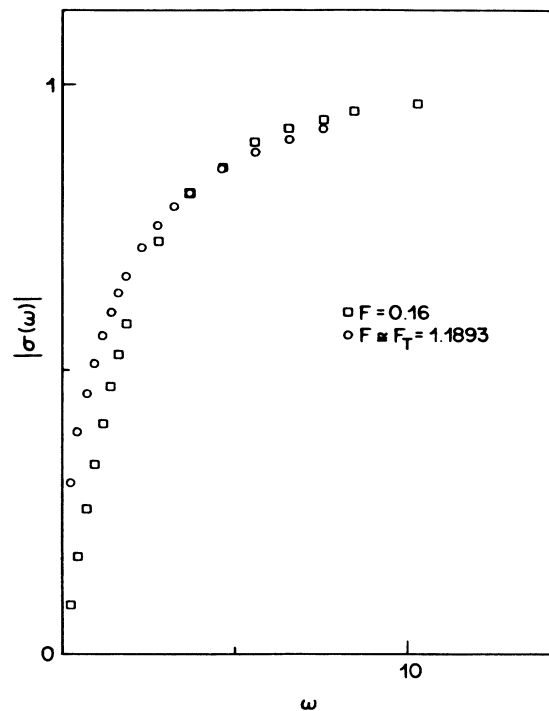


FIG. 8. Plots of the ac conductivity $|\sigma(\omega)|$ vs ω over a large range of frequencies for $F=0.16$ and $F \approx F_T$. Although the field changes the response for low frequencies, the qualitative features of the two curves are similar.

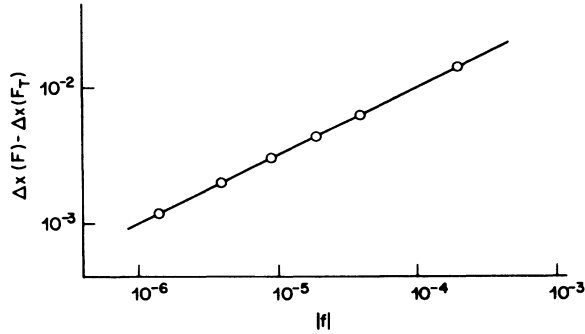


FIG. 9. Dominant gap $\Delta x(F)$ of the hull function for $F \lesssim F_T$; asymptotically, Δx appears to approach a finite value $\Delta x(F_T) = 3.71$ with an approximately square-root cusp. The line on the figure is a fit to this square-root form.

with $\Delta x(F_T) = 3.71076 \pm 0.00002$, $A = 0.975 \pm 0.02$, and $\nu = 0.5 \pm 0.03$. The value of Δ_0 in the absence of a field is 4.220599.

The divergence of the polarizability might have been expected to be associated with a diverging localization length of the low-lying eigenmodes. As mentioned above, this is not the case: the low-frequency modes remain well localized even at threshold. This is in contrast to the transition from the pinned to the unpinned phase as a function of potential strength V at $F=0$. In that case, as $V \rightarrow V_c^+$, the localization length of the lowest eigenmode diverges.

In the dynamical systems context where the extremal equations of the energy are interpreted as the “dynamics” of a particle with position x_j at “time” j , a useful quantity is the Lyapunov exponent λ_L which characterizes the divergence of trajectories from each other as time j is increased.¹⁰ The Lyapunov exponent λ_L can be expressed as the product of the eigenvalues

$$\lambda_L^{-1} = \frac{1}{p_n} \ln \prod_m \Lambda_m. \quad (3.7)$$

Here we calculate it using the method described by Greene.⁸ For $F=0$ the Lyapunov exponent has a value $\lambda_L^{-1} \approx 1.5$. This value decreases slowly as F increases until F approaches F_T , when it appears to approach a finite value with a sharp cusp. In contrast, for a finite system the inverse of the Lyapunov exponent must be $-\infty$ exactly at threshold, since it is the logarithm of the product of a finite number of terms, one of which is zero. Figure 10 shows log-log plots of $\lambda_L^{-1}(F) - \lambda_L^{-1}(F_T)$ versus $|f| = (1 - F/F_T)$ for a system of 144 particles. The value of F_T was not adjusted but rather it was taken to be the largest value of F for which a static solution to the force equations was obtained ($F_T = 1.18930533$). The three values of $\lambda_L^{-1}(F_T)$ that are shown are $\lambda_L^{-1}(F_T) = 0$, $\lambda_L^{-1}(F_T) = 0.66183925$ (which is the value obtained when $F = F_T$), and $\lambda_L^{-1}(F_T) = 0.6517138$. It is clear from the plot that the data is not fit well by the form $\lambda_L^{-1}(F) = A|f|^\delta$. Over more than four decades in $|f|$ the log-log plot of $\lambda_L^{-1}(F) - \lambda_L^{-1}(F_T)$ versus $|f|$ is linear with a slope very near $\frac{1}{6}$, though deviations are found for

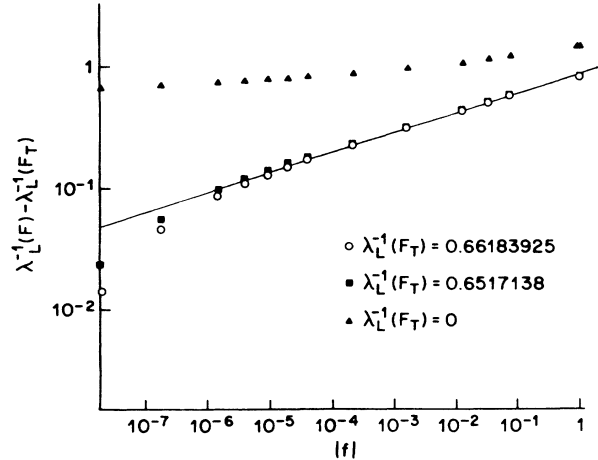


FIG. 10. Log-log plots of the Lyapunov exponent $\lambda_L(F) - \lambda_L(F_T)$ vs the reduced force $|f|$ for the three values $\lambda_L(F_T) = 0$ (triangles), $\lambda_L(F_T) = 0.6517138$ (squares), and $\lambda_L(F_T) = 0.66183925$ (circles), for a system with $p_n = 144$. The line on the plot corresponds to a slope of $\frac{1}{6}$. These plots indicate that λ_L appears to approach a finite value at $f=0$, as described in the text.

$|f| < 10^{-5}$. The choice $\lambda_L^{-1}(F_T) = 0.6517138$ improves the fit somewhat for small $|f|$, supporting the view that uncertainties in F_T and $\lambda_L^{-1}(F_T)$ could account for some of the discrepancy. Finite-size effects cannot account for the deviations, for the data for $p_n = 89$ and 144 differ by more than 5% only for $|f| < 10^{-7}$, but numerical errors are hard to estimate and may be larger than this result would indicate.

Though we cannot absolutely rule out the existence of a very weak singularity that causes λ_L to remain large even for very small $|f|$, the Lyapunov exponent has fallen by only a factor of 2.27 by the time $|f|$ is on the order of 10^{-8} . Therefore we believe that our data indicate that λ_L is not zero at F_T . Thus, in contrast to the transition at V_c for $F=0$, the Lyapunov exponent does not appear to

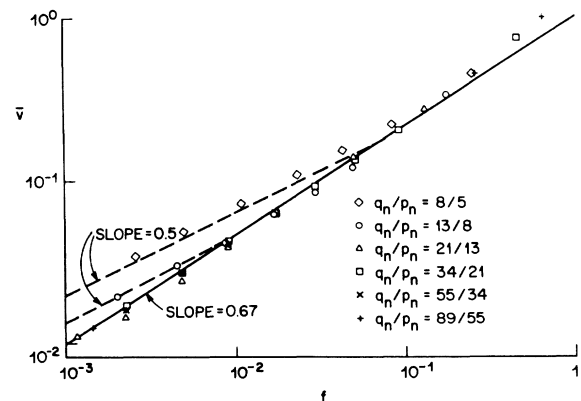


FIG. 11. Log-log plot of the mean velocity \bar{v} vs the reduced force f for different chain lengths, demonstrating that $\bar{v} \propto f^\zeta$, with $\zeta = 0.68 \pm 0.05$. The crossover to the one-particle behavior $\zeta = \frac{1}{2}$ is clearly visible for the smaller systems very close to threshold. The dashed lines have slope 0.5 and the solid line has slope 0.67.

yield a diverging length as $F \rightarrow F_T^-$. We shall see later, however, that there is another length which does diverge.

B. Behavior above threshold

For $F > F_T$, the steady-state velocity of the chain as a function of $f = (F - F_T)/F_T$ was calculated for $p_n = 5, 8, 13, 21, 34,$ and 55 . A log-log plot of the spatial and temporal mean velocity \bar{v} is shown in Fig. 11; the data are consistent with

$$\bar{v} \sim f^\zeta, \quad (3.8)$$

with $\zeta = 0.67 \pm 0.05$ for large sizes. As expected, the very small systems exhibit a crossover to the single-particle behavior, $\zeta = \frac{1}{2}$, very close to F_T , as seen in the figure. Thus an infinite number of degrees of freedom appear to induce a nontrivial velocity characteristic near threshold.

The time dependence of the spatially averaged velocity $v(t)$ was also examined. Figure 12 shows the (spatially averaged) velocity of a 21-particle system for $F = 1.20$ ($f \approx 0.009$) during one period of the motion. For this finite system close to threshold large oscillations occur, but they have period $2\pi/(p_n \bar{v})$ rather than the "washboard" period $T = 2\pi/\bar{v}$. The velocity of each particle $v_j(t)$ appears to be a 2π -periodic function of $\alpha j + \bar{v}t$, as in Eq. (1.8), and hence describable by a hull function g_+ . This description thus appears to be valid for both commensurate and incommensurate systems above threshold, which is consistent with the perturbation theory for large F .^{13,22} To understand this, one can imagine a system with an adjustable potential strength V moving at a fixed velocity \bar{v} . By simultaneously adjusting F and V , one can increase V from zero while keeping the velocity constant. The distortion in the position of each particle appears to depend only on V and on $\alpha j + \bar{v}t$, which was the position of the particle when the potential V was zero. This result is a continuation of the behavior observed for the stationary state at $F = F_T$; thus the hull function defined for

$F < F_T$ (Ref. 5) also exists for $F > F_T$, with only the modification from Eq. (1.3) to (1.8). This result implies that every particle moves identically except with a shifted origin of time, as found in our numerical results.

The magnitude of the oscillations in $v(t)$ as a function of system size were studied for $F = 1.20$ ($f \approx 0.9 \times 10^{-2}$) and $p_n = 21, 34,$ and 55 by calculating $\Delta v = (v_{\max} - \bar{v})/\bar{v}$, where v_{\max} is the maximum (spatially averaged) velocity attained in a period. As Fig. 13 shows, Δv decays to zero approximately as $1/p_n$ as p_n is increased, indicating that the velocity oscillations vanish in the incommensurate limit, and are thus a finite-size effect. These results supplement those of Sokoloff and Horowitz²³ and of Sneddon,²⁴ who have shown that velocity oscillations are absent in any finite order of perturbation theory in the potential for both incommensurate and random pinning, and they are consistent with mean-field theory, for which velocity oscillations are absent, and with general arguments.¹⁸ Recently, Sneddon and Cox²⁵ have discussed an instability of the average uniform motion if the system is driven at constant current. This instability appears to yield velocity oscillations in the infinite-volume limit. However, it does not occur in the voltage-driven configuration that we confine ourselves to here.

In order to further elucidate the form of the motion near threshold, the velocity of a given particle $v_j(t)$ was followed as a function of time and of position. Figures 14(a) and 14(b) show the velocity over one period for one particle of a 21-particle system with $F = 1.2$ ($f = 0.009$). The motion consists almost entirely of nearly discrete jumps. The largest velocity v_1^* is attained when the particle is hopping over a potential maximum, the next highest velocities v_2^* and v_2^* occur when an adjacent particle is jumping over a potential maximum, and so on. The v^* are each of order 1 and independent of f as $f \rightarrow 0$, but they appear to decay exponentially with distance from the particle hopping over the maximum. Although the jumping motion appears to be localized, the critical

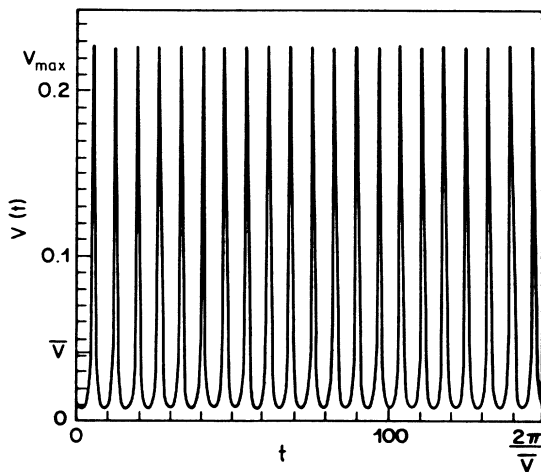


FIG. 12. Spatially averaged velocity $v(t)$ for $p_n = 21$ and $f = 8.99 \times 10^{-3}$. Large oscillations occur, but they have period $2\pi/p_n \bar{v}$ rather than the "washboard" period $2\pi/\bar{v}$.

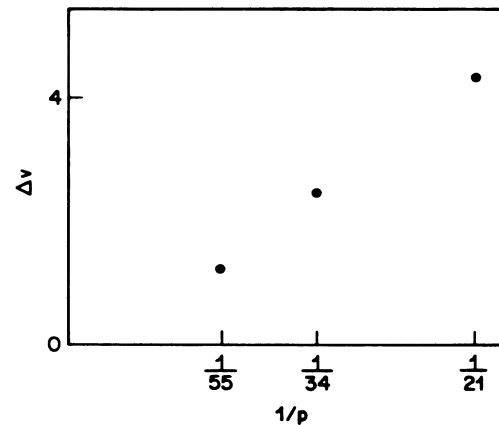


FIG. 13. Oscillation magnitude of the spatially averaged velocity $\Delta v = (v_{\max} - \bar{v})/\bar{v}$ for $f = 8.99 \times 10^{-3}$ and $p_n = 21, 34,$ and 55 . In this range the quantity Δv decays approximately as $1/p_n$ as p_n is increased.

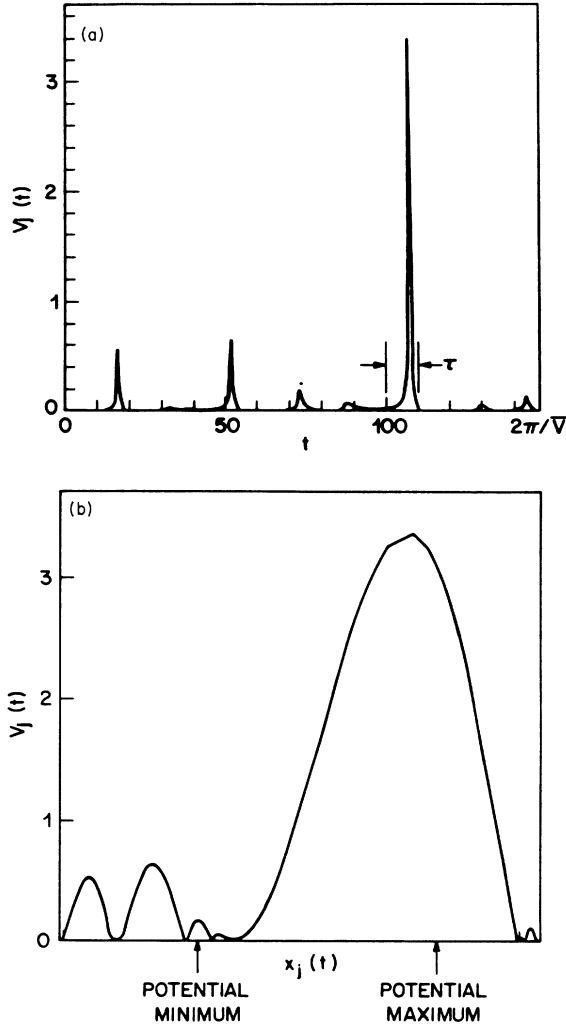


FIG. 14. (a) Velocity $v_j(t)$ of one particle of a 21-particle system for one period with $V=4$ and $F=1.2$. The particle attains a velocity of order unity while hopping over a maximum of the potential, but most of the time it moves very slowly. (b) Velocity of the same particle plotted as a function of its location x_j over one period. This graph demonstrates that almost all the distance it travels is covered during "jumps."

behavior is nontrivial because there are many widely separated regions jumping simultaneously. The peaks in the spatially averaged velocity each correspond to some particle jumping over a potential maximum, and for small f , the spatially averaged v_{\max} is very nearly equal to $(v_1^* + v_2^* + v_3^*)/p_n$. Since the v^* are independent of f as f tends to zero, v_{\max} decays like $1/p_n$ as p_n is increased, approximately as observed.

For large enough p_n at any fixed $f > 0$, there will be several particles each moving fast at any time. This causes a more rapid decay of the size dependence of Δv : we expect exponential (or faster) decay with p_n due to the smoothness of the hull function g_+ . The crossover between these regimes as well as the finite-size effects on the average velocity are subtle and we will not delve into them here.

IV. SCALING LAWS AND INTERPRETATION OF RESULTS

It is clear that the critical behavior exhibited near the threshold transition is quite unusual. The localization length and the dominant gap in the hull function both stay of order unity as the force approaches the threshold from below. This situation is in contrast to the pinning transition for $F=0$ and $V=V_c$, at which the localization length is infinite and the gaps in the hull function vanish. However, it is clear that in spite of the absence of divergences in some of the quantities, the threshold does have a continuous critical nature, since the velocity goes continuously to zero at the transition and just above threshold the entire chain moves without hysteresis at a steady-state velocity.

The dominant feature appears to be well-separated localized "active" regions that occur on either side of the threshold. For $F < F_T$ these regions correspond to the low-frequency eigenmodes, and for $F > F_T$ they correspond, at a given time, to the jumping regions. The localization length corresponds to the size of each active region, but another length scale is needed to describe the typical distance between active regions. Although the width of the jumping regions remains finite (and quite small), for $F \rightarrow F_T^+$ the separation between jumping regions diverges as f tends to zero.

The results can be described in terms of two nontrivial exponents, one for the behavior of each active region and the other for the density of active regions. For $f < 0$, the spectrum can be roughly written in the scaling form

$$\Lambda_m \sim f^\mu D(m/f^\delta), \quad (4.1)$$

where Λ_m is the eigenvalue of the m th eigenmode. It is clear from Fig. 3 that the scaling function D is not smooth, but this does not preclude the existence of a scaling form. The function D would be invariant under discrete scale changes, though not continuous ones, and would thus exhibit self-similarity. Figure 15 shows a plot of Λ_m as a function of m for different values of the reduced force f for a system of 144 particles. The eigenvalues Λ_m are well described (to within about 25%) of the form

$$\begin{aligned} \Lambda_m(f) &= \Lambda_m(f=0) \quad [\Lambda_m(f=0) > Af^\mu] \\ &= Af^\mu \quad [\Lambda_m(f=0) < Af^\mu], \end{aligned}$$

with $A=3.4$. The exponent μ describes the scaling of the frequency of the softest modes. Thus the scaling form holds if the frequencies of the modes exactly at threshold are described by a scaling form with the exponent δ describing the soft-mode density; in one dimension δ would correspond to a correlation length exponent. The numerical results for the phonon eigenvalues do not provide convincing evidence that they scale because numerical limitations of our diagonalization routines prevent the accurate determination of the eigenvalues down to very low values. However, over a fairly narrow range of frequencies (roughly two orders of magnitude), scaling appears to be obeyed.

For calculating the polarizability and the ac conduc-

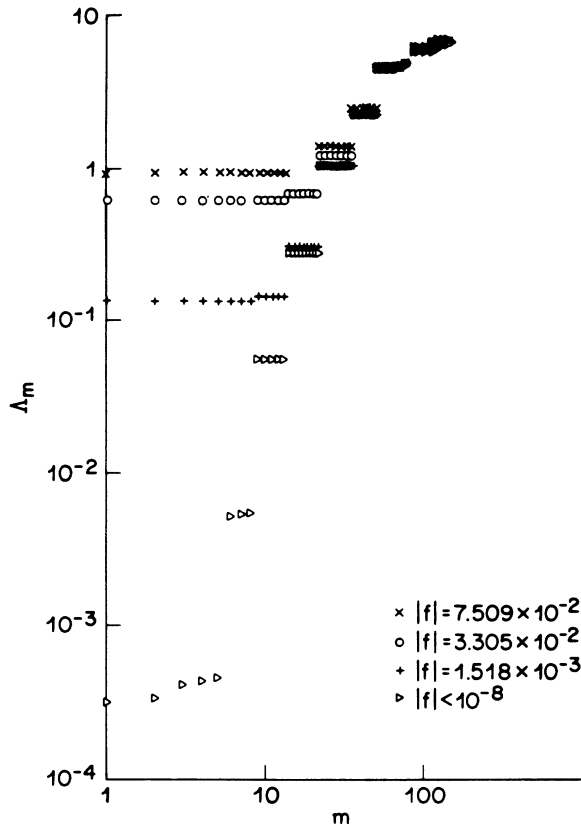


FIG. 15. Plot of the eigenvalues Λ_m vs m for $p_n=144$ and $f = -7.509032 \times 10^{-2}$, -3.3049×10^{-2} , -1.5180×10^{-3} , and 0 (less than 10^{-8}). This plot is consistent with the scaling behavior of the eigenvalues, as discussed in the text.

tivity, the uniform part of the eigenvectors, $\sum_j u_m(j)$, is needed [see Eq. (3.7)]. Empirically, $\sum_j u_m(j)$ tends to a constant for all small m . This observation reflects the fact that the soft modes correspond to particles that are about to hop over potential maxima and therefore primarily involve forward motion. If the scaling form Eq. (4.1) is correct, the polarizability exponent should satisfy

$$\gamma = \mu - \delta, \quad (4.2)$$

and the exponent ρ of the ac conductivity at threshold should obey

$$\rho = \delta / \mu. \quad (4.3)$$

Since μ can be measured directly from the lowest eigenvalue, Eq. (4.2) and (4.3) comprise a nontrivial test of the scaling relations. The observed values $\rho = 0.35 \pm 0.05$ and $\gamma = 0.34 \pm 0.02$ are both consistent with $\mu = \frac{1}{2}$ and $\delta = \frac{1}{6}$.

Straightforward application of the scaling argument to the F dependence of the Lyapunov exponent λ_L [Eq. (3.7)] yields the expectation that λ_L^{-1} approaches a constant at $F = F_T$, with the leading correction proportional to $|f|^{1/6} \ln(|f|)$. The numerical results are consistent with this expectation.

In the moving phase, a similar but more heuristic argument can be made. Even though a particle attains a velocity of order 1 during a jump, the time it takes to accelerate should diverge as f tends to zero, so a time scale

$\tau \propto f^{-\mu}$ is associated with the time it takes to complete a jump (this behavior is found in mean-field theory^{18,19}). In Fig. 14(a) the jump time can be defined as that required to travel between successive velocity minima, as delineated by the arrows. As f tends to zero, however, the average velocity of the chain is reduced so that more and more minima appear (corresponding to the completion of jumps of particles that are farther and farther away), so it is numerically quite difficult to calculate this time scale accurately. However, in the asymptotic limit ($f \rightarrow 0$), the jumping time scale is well-defined to within constant factors, and we make the natural guess that it follows the same power-law behavior as the time scale of the softest mode below threshold. We also assume that the density of hopping regions scales as f^δ , just as the density of soft modes scales below threshold. If these assumptions hold, then the mean velocity of the chain \bar{v} satisfies $\bar{v} \propto f^{\mu+\delta}$; in other words,

$$\zeta = \mu + \delta. \quad (4.4)$$

This argument assumes both that the jumping regions dominate the asymptotics so that slow drift of the chain can be neglected, and that the exponents are identical above and below threshold. The measured value of ζ is consistent with this scaling law, but as mentioned above it is very difficult numerically to evaluate μ separately as was done for $f < 0$, since this would involve separating the jumping velocity from the drift velocity, a procedure which is well defined only in the $f \rightarrow 0$ limit. Therefore, although the agreement is very suggestive, the applicability of this scaling law is by no means certain.

Note that if the scaling laws Eqs. (4.2)–(4.4) are valid, the number of independent exponents is reduced from four to two. For a finite number of degrees of freedom we have $\delta = 0$ and $\mu = \frac{1}{2}$, consistent with all the scaling laws.

Our scaling postulates are rather unlike ordinary critical phenomena scaling because of the existence of two time scales that diverge with different exponents, $\bar{v}^{-1} \sim f^{-\zeta}$ and $\Lambda_0^{-1} \sim f^{-\mu}$. In addition, some of the finite-size effects also enter in a rather weak way: the dependence of the threshold force on system size (Sec. III) is not a power of p_n , in contrast to what might have been expected. This may be because of the special choice of the optimal rational approximants to the incommensurate chain. As for the size dependence of the time-averaged velocity, the crossover between $\zeta = 0.67$, characteristic of the infinite system, and $\zeta = 0.5$, typical of the one-particle system, can be estimated from the data of Fig. 11 for systems with 5, 8, and 13 particles. The value of f at which the crossover occurs shrinks by roughly an order of magnitude for each succeeding approximant. This result is roughly consistent with finite-size scaling, where one would expect the value of f at which the crossover occurs to scale as $p_n^{1/8}$, yielding a factor of about 17 between successive rational approximants.

A. Comparison with mean-field theory

The mean-field theory studied by one of us^{18,19} exhibits features that appear to be consistent with the scaling

scenarios discussed above, but there are complications arising from jumping between various metastable states as the force is varied below threshold. The simplest mean-field case is that with identical pinning strengths V_j in Eq. (1.13). For this case, it is possible to define linear response below threshold without jumps between metastable energy minima, and then the scaling postulated above holds with the exponents $\mu = \frac{1}{2}$ and $\delta = 1$. However, the singularity in the polarizability described by an exponent of $\gamma = -\frac{1}{2}$ from Eq. (4.2) is only a subdominant singularity. This problem arises because the polarizability does not diverge for F approaching F_T from below; rather it jumps discontinuously from a finite value to infinity at $F = F_T$, which can be described by an exponent $\gamma = 0$. For any type of bounded random distribution of pinning strengths, the critical behavior for $F > F_T$ is unambiguously characterized; $\zeta = \frac{3}{2}$ and $\mu = \frac{1}{2}$ are both obtained analytically and are independent of details. The results in the moving phase are consistent with the scaling law Eq. (4.4) and with the picture in terms of jumps, although the exponent δ cannot be interpreted in terms of a length.

The dominant feature of mean-field theory below threshold is the presence of metastable states and the nonuniversality of the polarizability because of jumping between different metastable minima. Our investigations of the one-dimensional incommensurate system have been designed to avoid this behavior, although study of the metastable states is certainly possible in the incommensurate system.

Comparison with mean-field theory can yield insight into which features of the incommensurate chain will generally hold for large pinned systems. The localized nature of the phonon excitations, the hopping just above threshold, and the absence of velocity oscillations in the infinite-size limit are all characteristic of both mean-field theory and incommensurate pinning in one dimension. However, although metastable states are present for the chain, in contrast to mean-field theory they do not affect the linear response of the state that evolves from the $F=0$ ground state for forces below the threshold value. It is expected that the threshold forces of the other metastable states will be lower than the F_T calculated here and they will evolve discontinuously to different metastable states at their thresholds. As F_T is approached, all the metastable configurations which still exist will be similar to the state we have investigated on a length scale that diverges at threshold. We conjecture that this characteristic length scale will diverge as $|f|^{-\delta}$. For more general pinning distributions, jumps between metastable states as F is increased are expected to be important for *all* initial configurations at $F=0$, so in this regard the mean-field theory probably is more realistic. For further discussion of the mean-field-theory results and their relevance to real CDW's, the reader is referred to the discussion in Ref. 18.

V. DISCUSSION

It is clear that an incommensurate harmonic chain displays unusual critical properties near threshold. The

phonons remain localized even at threshold, yet there is some sort of long-range coherence, since the entire system starts to move at threshold. The velocity characteristic near threshold is markedly different from that of one particle in a sinusoidal potential (i.e., zero dimensions) and that of the mean-field theory. The motion just above threshold is dominated by incoherent hops across maxima in the potential, and uniform velocity oscillations appear to be absent in the infinite system limit.

The results for zero dimensions, one dimension, and the mean-field theory (infinite dimension) appear to indicate a trend that ζ increases as the dimensionality of the system is raised. This expectation is consistent with experiments on three-dimensional charge-density wave systems, for which $\zeta > 1$ is needed to fit experiments, since $d\bar{v}/dF$ vanishes as $F \rightarrow F_T^+$.²⁶ The nontrivial exponent ζ characterizing the velocity near threshold reflects the interactions of infinitely many degrees of freedom.

Comparison with previous work on related models^{19,23,24} indicates that the absence of velocity oscillations in the infinite limit may be a general feature of the model Eq. (1.12) in the absence of a commensurate potential. The jerky motion of individual particles found near threshold also appears prominently in mean-field theory as well as in numerical simulations of randomly pinned systems.¹⁴⁻¹⁶ Both these conclusions are relevant to observations on sliding charge-density waves.

Studies with different incommensurate particle densities and potential strengths would certainly be worthwhile, but we expect that the absence of velocity oscillations, the unusual polarizability and ac conductivity, and the nontrivial velocity exponent will be general features of incommensurate pinning. In analogy to previous work on the pinning transition of the discrete sine-Gordon equation, the universality of the exponents as the commensurability α is varied is an interesting question. However, the numerical accuracy of the exponents obtained here is insufficient to distinguish differences on the order of a few percent (the amount by which the exponents vary for different α in the pinning transition that occurs as a function of V),²⁰ so we have not attempted such a study.

A renormalization-group description of the critical behavior of ours and similar models does not appear to be easy because of the existence of two separate diverging time scales, as discussed above. In addition, there is a prominent microscopic length scale, corresponding to the dominant gap at threshold (the distance the particle hops when it jumps across a potential maximum). Therefore a rather subtle renormalization-group description is needed.²⁷

An interesting question concerns the role of inertia in the threshold behavior of these types of systems, since all the calculations described here were done using purely dissipative dynamics. A large mass almost certainly can drive the threshold transition first order [with a hysteresis $\bar{v}(F)$], as can be seen by looking at the one-particle case as well as perturbation theory for very large mass. However, if inertia is an irrelevant variable in the renormalization-group sense, the results obtained here should apply to the more general case of a system with

small but finite inertia.

For the one-particle case, a small mass does not drive the transition first order as long as the potential has a continuous first derivative, but for some discontinuous potentials an arbitrarily small inertia can drive the transition first order. However, for the many-body case we are mainly concerned with smooth potentials. Since fast moving regions become very far apart near threshold, it is reasonable that, in general, the addition of collective couplings to the single-particle case does not enhance the inertial effects. In mean-field theory it has indeed been shown that small inertia is irrelevant.¹⁸ However, no definitive calculation has been done for the incommensurate case discussed here.

Experimentally, for charge-density waves the inertia, as measured using the ac conductivity in zero field, has been shown to be entirely negligible up to frequencies on the order of 10 GHz.²⁸ Some nonlinear effects which might appear to be due to inertia have been observed,²⁹ but they have been shown to be compatible with the purely dissipative equation of motion such as that studied here.³⁰ Therefore it is entirely reasonable to neglect inertial terms in the equation of motion for CDW systems. We note, however, that some samples do exist which exhibit first-order threshold transitions with hysteresis, for which models such as those studied here are inadequate.³¹ These discontinuities probably reflect tears in the CDW, and the effects of dislocations must be taken

into account.³²

Another effect neglected in the modes discussed here is thermal fluctuations. In one dimension the effects of finite temperature on the behavior of the incommensurate chain are expected to be rather large. As in other one-dimensional systems, thermal fluctuations will always be relevant. Here they will cause slow creep in the presence of applied forces of any strength. However, the crossover between creep and sliding is expected to remain fairly sharp at low temperatures, as in mean-field theory.^{18,19} Investigations of finite temperature effects in one dimension should be very interesting. Although thermal creep effects have been argued to be negligible in sliding CDW's, they can play a much larger role in flux lattice flow in superconductors.^{3,18}

In conclusion, we have investigated the threshold behavior of a one-dimensional incommensurate harmonic chain. We find that it is described by critical exponents that are different from both those of mean-field theory and zero dimensions. We have proposed scaling relations that are compatible with these results and which further support the view that the threshold process is a novel dynamic critical phenomenon where the nonlinear dynamics of an infinite number of degrees of freedom plays an essential role. However, full understanding of the threshold critical behavior via the renormalization group is still needed.

*Present address: Department of Physics, Princeton University, Princeton, NJ 08544.

¹See, for example, J. Guckenheimer and P. Holmes, *Nonlinear Oscillations, Dynamical Systems, and Bifurcations of Vector Fields* (Springer-Verlag, Berlin, 1983).

²See, e.g., *Spatio-Temporal Coherence and Chaos in Physical Systems*, edited by A. R. Bishop, G. Gruner, and B. Nicolaenko [Physica D **23** (1986)].

³D. S. Fisher, in *Nonlinearity in Condensed Matter*, edited by A. R. Bishop, D. K. Campbell, P. Kumar, and S. Trullinger (Springer-Verlag, New York, 1987), and references therein.

⁴S. N. Coppersmith, Phys. Rev. B **30**, 410 (1984).

⁵S. Aubry, in *Solitons and Condensed Matter Physics*, Vol. 8 of *Springer Series in Solid-State Sciences*, edited by A. R. Bishop and T. Schneider (Springer, Berlin, 1978), p. 264.

⁶R. B. Griffiths and W. Chou, Phys. Rev. Lett. **56**, 1929 (1986); W. Chou and R. B. Griffiths, Phys. Rev. B **34**, 6219 (1986), and references therein.

⁷I. Niven, *Irrational Numbers* (Mathematical Association of America, Menasha, WI, 1979).

⁸J. M. Greene, J. Math. Phys. **20**, 1183 (1979); **9**, 760 (1968).

⁹S. N. Coppersmith and D. S. Fisher, Phys. Rev. B **28**, 2566 (1983). See also M. Peyrard and S. Aubry, J. Phys. C **16**, 1593 (1983).

¹⁰S. J. Shenker and L. P. Kadanoff, J. Stat. Phys. **27**, 631 (1982).

¹¹R. S. MacKay, Ph.D. thesis, Princeton University, 1982.

¹²This result can be obtained by a straightforward generalization of the perturbation theory at $V=0$ and is also supported by unpublished numerical work of L. Sneddon.

¹³L. Sneddon, Phys. Rev. Lett. **52**, 65 (1984).

¹⁴N. Teranishi and R. Kubo, J. Phys. Soc. Jpn. **47**, 720 (1979); H. Matsukawa and H. Takayama, Solid State Commun. **50**, 282 (1984).

¹⁵J. Sokoloff, Phys. Rev. B **23**, 1992 (1981); **31**, 2270 (1985).

¹⁶P. B. Littlewood, Phys. Rev. B **33**, 6694 (1986).

¹⁷H. Fukuyama and P. A. Lee, Phys. Rev. B **17**, 535 (1978); P. A. Lee and T. M. Rice, *ibid.* **19**, 3970 (1979).

¹⁸D. S. Fisher, Phys. Rev. B **31**, 1396 (1985).

¹⁹D. S. Fisher, Phys. Rev. Lett. **50**, 1486 (1983).

²⁰S. N. Coppersmith, Ph.D. thesis, Cornell University, 1983.

²¹L. Sneddon, Phys. Rev. B **30**, 2974 (1984).

²²L. Sneddon, M. C. Cross, and D. S. Fisher, Phys. Rev. Lett. **49**, 292 (1982).

²³J. B. Sokoloff and B. Horovitz, J. Phys. (Paris) Colloq. **44**, C3-1667 (1983).

²⁴L. Sneddon, Phys. Rev. B **29**, 719 (1984).

²⁵L. Sneddon and K. A. Cox, Phys. Rev. Lett. **58**, 1903 (1987).

²⁶See, e.g., P. Monceau, M. Renard, J. Richard, M. C. Saint-Lager, and Z. Z. Wang, *Charge Density Waves in Solids*, Vol. 217 of *Lecture Notes in Physics*, edited by G. Hutiray and J. Solyom (Springer-Verlag, Berlin, 1985), p. 279.

²⁷P. B. Littlewood and C. M. Varma, Phys. Rev. B **36**, 480 (1987), have made an attempt in this direction by renormalizing the pinning potential as well as the length and frequency for a three-dimensional randomly pinned elastic medium. L. Sneddon, S. Liu, and A. J. Kassman (unpublished), have constructed a renormalization group analogous to one that can be used for the zero-force transition. They were unable to find a nontrivial fixed point using this method, which is further evidence that straightforward extension of previous

- methods is not adequate.
- ²⁸S. Sridhar, D. Reagor, and G. Grüner, *Phys. Rev. Lett.* **55**, 1196 (1985).
- ²⁹G. X. Tessema and N. P. Ong, *Phys. Rev. B* **31**, 1181 (1985); S. E. Brown, G. Mozurkewich, and G. Grüner, *Phys. Rev. Lett.* **52**, 2277 (1984).
- ³⁰S. N. Coppersmith and P. B. Littlewood, *Phys. Rev. B* **31**, 4049 (1985).
- ³¹P. Monceau, J. Richard, and M. Renard, *Phys. Rev. B* **25**, 931 (1982); R. P. Hall, M. Sherwin, and A. Zettl, *Phys. Rev. Lett.* **52**, 2293 (1984).
- ³²M. Inui, R. P. Hall, S. Doniach, and A. Zettl (unpublished).